Drug Discovery

To Cite:
Aghahowa S, Ozolua R, Bafor E, Isah A, Aghahowa M, Osifo D, Obarisiagbon P, Aikorogie P. Metabolomics of Artemisinin-Based Combination Therapies in experimental animals and humans. *Drug Discovery* 2026; 20: e1dd3033
doi:

Author Affiliation:
[1]Department of Pharmacology and Toxicology, University of Benin, Nigeria
[2]Department of Clinical Pharmacology and Therapeutics, University of Benin, Nigeria
[3]Department of Surgery, College of Health Sciences, Nile University of Nigeria, Abuja, Nigeria
[4]Department of Surgery, College of Medical Sciences University of Benin, Nigeria
[5]Department of Chemical Pathology, University of Benin Teaching Hospital Benin City, Nigeria

[*]**Corresponding Author**
Aghahowa S.E
Department of Pharmacology and Toxicology,
University of Benin, Benin City, Nigeria.
Email: se-aghahowa@uniben.edu
Tel:+234 805 5219550.
http://orcid.org/0000-0001-6627-239X

Peer-Review History
Received: 07 July 2025
Reviewed & Revised: 21/July/2025 to 16/December/2025
Accepted: 21 December 2025
Published: 03 January 2026

Peer-Review Model
External peer-review was done through double-blind method.

Drug Discovery
pISSN 2278–540X; eISSN 2278–5396

Metabolomics of Artemisinin-Based Combination Therapies in experimental animals and humans

Sylvester Aghahowa[1*], Raymond Ozolua[1], Enitome Bafor[1], Ambrose Isah[2], Michael Aghahowa[3], David Osifo[4], Philip Obarisiagbon[1], Paul Aikorogie[5]

ABSTRACT

Due to the limited metabolomic data of Artemisinin-Based Combination Therapies (ACTs) in endemic regions, the study assessed the metabolomics of recommended ACTs to understand the pattern of adverse effects in experimental animals (mice, rats, guinea pigs, rabbits) and humans using mass spectrometry. Malaria infection was simulated in all the animal models using *Plasmodium berghei NK65*, patients who had *Plasmodium falciparum* infection were also selected. ACTs were administered orally in conventional doses. Serum samples were collected and assayed for metabolomic parameters using standard protocols. The most common metabolites that were significantly altered metabolites in all the models were D-glucose, creatinine, glutamate, aspartate, glycine, taurine, eicosapentaeinoyl-glycerol, hexadecanoic acid, amino-butanoate, and L-tyrosine (OPLS-DA). Commonly altered pathways were lipid, amino acid, carbohydrate, and nucleotide (OPLS-DA). Statistical changes in the values of prediction/correlation in models were 0.77/1 (rats):0.72/0.98 (humans):0.57/1 (guinea pigs):0.27/0.79 (mice):and -0.14/0.54 (rabbits) (OPLS-DA). Sulphadoxine, pyrimethamine, and artemisinin were the commonly expressed drugs significantly in all the models (OPLS-DA). Variations in the values of prediction/correlation of ACTs in humans and animals were (AL ≥ AA > AM > ASP >DHP) and (AL > AA > AM > DHP> ASP): respectively. The annotated metabolomic study had shown that ACTs altered metabolites and metabolic pathways. The results therefore suggest caution in the selection of ACTs in malaria therapy due to possible induction of toxicities.

Keywords: Metabolomics, ACTs, Malaria, Mass spectrometry, Multivariate analysis, Toxicity.

1. INTRODUCTION

There are reports that about one hundred countries or territories in the world have been identified to be endemic regions. Almost half of these countries are in the sub-Saharan Africa (WHO, 2013). This number seems to be considerably less compared to what have been reported in the mid-1950s, and in about 140 countries or territories globally. Meanwhile, more than 2.4 billion of the world's population are still at risk (WHO, 2013). Artemisinin–Based Combination Therapies have been recommended

for the treatment of uncomplicated malaria(WHO, 2001). Nigeria adopted the use of Artemether-Lumenfantrine as a first-line drug and Artesunate-Amodiaquine as alternative (FMOH, 2005). Adverse effects, high cost and inaccessibility have been reported as drawbacks in the use of ACTs (Falade and Manyando, 2009; WHO,2013; Bassi *et al.,* 2013; Aghahowa *et al.,* 2014). Limitations observed in past studies showed that few ACTs have been evaluated for efficacy and toxicity (Falade *et al*., 2009). The use of subjective instruments such as questionnaires and case-data forms has been over-explored (Bassi *et al.,* 2013; Aghahowa *et al.,* 2014). Also, routine pre-clinical safety evaluation (Falade *et al*., 2009; Aprioku and Obianime, 2011) were adopted rather than advanced technologies. Metabolomic phenomena have been defined as the comprehensive analysis of the small molecules in a biological system under a given set of conditions (Fiehn, 2001). Metabolomics methods are usually combined with chemoinformatics approaches such as unsupervised multivariate analysis methods, to unravel interesting variation in the groups of biological samples, by taking note of their *m/z* values for mass spectrometry data, and chemical shifts for Nuclear Magnetic Resonance data (Boroujerdi *et al*.,2009). Since metabolomic studies of ACTs are lacking, the studies can identify some metabolites such as lipids, carbohydrates, amino acids, xenobiotics, and related analogues that are indicators of efficacy and toxicity studies (Want *et al.,* 2006; Dun *et al.,* 2011; Bouhifd *et al.,* 2013). These indicators are regarded as complex moieties and stressors (Want *et al.,* 2006; Dun *et al.,* 2011; Bouhifd *et al.,* 2013) that may alter a biological system. Metabolomics is now commonly applied in drug discovery and development (Bafor *et al.,* 2017; Bafor *et al.,* 2018):also to strengthen the existing profile reports of new therapies. The study evaluates the metabolomics of Artemisinin-Based Combination Therapies to identify the possible metabolites and pathways that may be of influence to efficacy and toxicity in laboratory animals (mice, rats, guinea pigs, rabbits):and humans.

2. MATERIALS AND METHODS

The study centres were the Department of Pharmacology and Toxicology, University of Benin, Nigeria and the University of Benin Teaching Hospital, Benin City, Nigeria. The collaborating centre was the Institute of Pharmacy and Biomedical Science, University of Strathclyde, Glasgow United Kingdom. Ethical approval (*ADM/E 22/A/VOL VII/1047*) was obtained from the Animal Ethics Committee of the University of Benin, Nigeria for the animal-based studies. Also, the ethical approval (*EC/FP/015/05*) was sought and got from the University of Benin Teaching Hospital Benin City, Nigeria, for the human-based studies.

Table 1. The (ACTs) used and the dosing regimen as recommended (WHO, 2001)

ACTs	fixed-dose combination	mg/kg body weight
Arthemeter/lumefantrine	20/120 mg	1.7/12
Artesunate/amodiaquine	50/135 mg	4/10
Artesunate/mefloquine	50/250 mg	4/8.3
Artesunate/sulfadoxine/pyrimethamine	50/500/25 mg	4/70/3.5
Dihydroartemisinin/piperaquine	40/320 mg	4/18

Fixed-dose combination of ACTs computed in mg/kg body weight used in all the models

The fixed-dose combination tablets were administered orally by the patients in mg/kg body weight while the powder samples of individual drugs were prepared and given orally as combinations to all the experimental animals in mg/kg body weight. These ACTs were sourced directly from registered pharmacies in Benin City, Nigeria and the powders of ACTs used for the experimental animals were sourced through Edo Pharmaceuticals Limited, Benin City, Nigeria. The sample sizes and the groupings were adapted (Mathur-De, 2000; Want *et al.,* 2006; WHO, 2007; Bouhifd *et al.,* 2013).

Experimental protocol for the experimental animals (mice, rats, guinea pigs, and rabbits)

The experimental animals (mice, rats, guinea pigs, rabbits) of both sexes were selected and handled during the study in accordance with the National Institute of Health guide regarding the care and the use of laboratory animals (NIH, 2011). The animals were infected with *Plasmodium berghei NK65* by snipping the tail tip of an infected mouse sourced from the Nigerian Institute of Pharmaceutical Research and Development, Abuja Nigeria. About 2-3 drops of infected blood extracted from the snipped tail of the mouse was diluted with 0.9 ml of sterile saline (0.9% NaCl). The animals were inoculated intraperitoneally using 0.1 ml of the diluted parasitized saline suspension as previously described (Fidock *et al.,* 2004; Xie *et al.,* 2006; Krettli *et al.,* 2009). The raw anti-malarial powder drugs were dissolved in *olive oil* a as vehicle and administered in mg/kg body weight using an oro-gastric tube to the treated groups, while 0.5 ml of

the vehicle was administered to the control group. The prepared drugs were administered 12 hourly for Artemether/lumfantrine, Artesunate/amodiaquine, Dihydroartemisinin/piperaquine in mg/kg body weight, and 24 hourly for Artesunate/sulphadoxine/pyridoxine, and Artesunate/mefloquine in mg/kg body weight for three days according to the standard regimen (WHO, 2001). On the fourth day, the rats were euthanized using chloroform anaesthesia and blood samples of 5-8 ml were withdrawn from the abdominal aorta as in previous reports (Flecknell, 1996). The blood samples were transfered into plain bottles.

Experimental protocol for humans

Selected patients were given informed consent to fill in accordance with standard guideline (WHO, 2010). Those that agreed after filling the consent form, were randomly allotted into five groups. The ACTs were given freely to all the participants for them to administer orally. Blood samples of 5-7 ml were withdrawn from the ante-cubital vein of each patient before and after the completion of treatment; that was on Day 0 and Day 4 respectively. All information about the patients who participated was kept confidential.

Metabolite extraction and mass spectrometry

Standard protocol for extraction of sera was carried out as in recommended procedures (Cheng *et al.*, 2015). Blood samples collected from both animals and humans were introduced into plain bottles as reported specifications (Want *et al.*, 2006). These samples were allowed to clot at room temperature to get a clear sera before centrifugation using the Hettich centrifuge (Rototix 32A, Germany) at 3500 rpm/g for 10 minutes. The sera extracted were stored in plain containers at temperature of -80 °C. These samples were sent in ice-pack maintained in cold chain until arrival at the Institute of Pharmacy and Biomedical Science, University of Strathclyde, Glasgow United Kingdom. Each fluid sample was freeze-dried in a freeze-drier (Christ Alpha 2-4, SciQuip, UK): and weighed. Hexane, acetonitrile, and water were added as extracting solvents in a ratio of 1:1:1 according to the procedure specified (Cheng *et al.*, 2015). The mixture was vortexed for 2 minutes using a vortexing apparatus (*Sciquip*$^{(R)}$ USA) to ensure adequate homogenous mixing of the solvents. The content of the cloudy solution was separated by centrifugation at 3500 rpm for 20 min. The resulting solution separated into three phases as hexane on top, acetonitrile/water at the middle and the precipitate of protein at the bottom. One milliliter of the separated polar and non-polar phases was withdrawn into labeled High Performance Liquid Chromatography (HPLC) vials for the assay. All reagents used were of analytical grade and were purchased from Fisher Scientific, Hemel Hempstead, UK. The HPLC-grade water was generated in-house from a direct Q-3 water purification system (Millipore, Watford, UK). The samples were arranged in HPLC rack as blank solvent, positive control, and test groups. Experimental steps were carried out as described (Cheng *et al*., 2015): using an Exactive mass spectrometer with an electrospray ionization source attached to an Accela 600 HPLC pump with Accela autosampler, and UV/Vis detector (Thermo Scientific, Bremen Germany). The mass accuracy was regulated to be less than 3.0 ppm. Meanwhile, the Orbitrap mass analyzer was able to limit the mass error within ±3.0 ppm. The instrument was calibrated in order to maintain a mass accuracy of ±1.0 ppm by applying the lock mass function as described in previous procedure (Cheng *et al.*, 2015). The instrument was externally calibrated according to the manufacturer's instructions before the run and was internally calibrated during the run using lock masses. In positive ion mode, the lock masses were *m/z* 83.06037 (acetonitrile dimer) and in the negative ion mode the lock mass was *m/z* 91.00368 (formic acid dimer). Mass spectrometry was carried out over a mass range between 100 and 2000 *m/z* in positive and negative ionization modes having spray voltage of 4.5 kV and capillary temperature at 270 °C. The volume of 10 microlitre of sample was injected into each vial, at a flow rate of 300 µL/min. The column used was an ACE5 C18 column (5 µm × 75 mm × 3 mm) (Hichrom Limited, Reading, UK). A binary gradient method was utilized. The use of two solvents A (water and 0.1% formic acid) and B (MeCN and 0.1% formic acid) represent the binary gradients utilized. The gradient was carried out for 45 minutes and the program was in the following order. At zero minutes, A = 90% and B = 10%; at 30 min, A = 0% and B = 100%; at 36 min, A = 90% and B = 10%; until end at 45 min. The UV absorption wavelength was programed at 254 nm, the sample tray temperature was maintained at 4 °C and the column maintained at 20 °C. The samples were analysed sequentially using solvent and media blanks at the beginning. The LC-MS data were acquired using Xcalibur version 2.2 (Thermo Scientific, Bremen, Germany). Fragment mass tolerance for molecular formula detection was programmed at ±5 ppm as in procedures (Macintyre *et al.*, 2014).

Data analysis for mass spectrometry

Data processing was adapted as in previous studies (Wishart *et al.*, 2007; Macintyre *et al.*, 2014). The resulting raw LC-MS data were initially sliced by the MassConvert tool ProteoWizard into positive or negative files in the mzML format (Fig.1). The sliced datasets were imported into MzMine 2.12, which is a framework for differential analysis of mass spectrometry data.

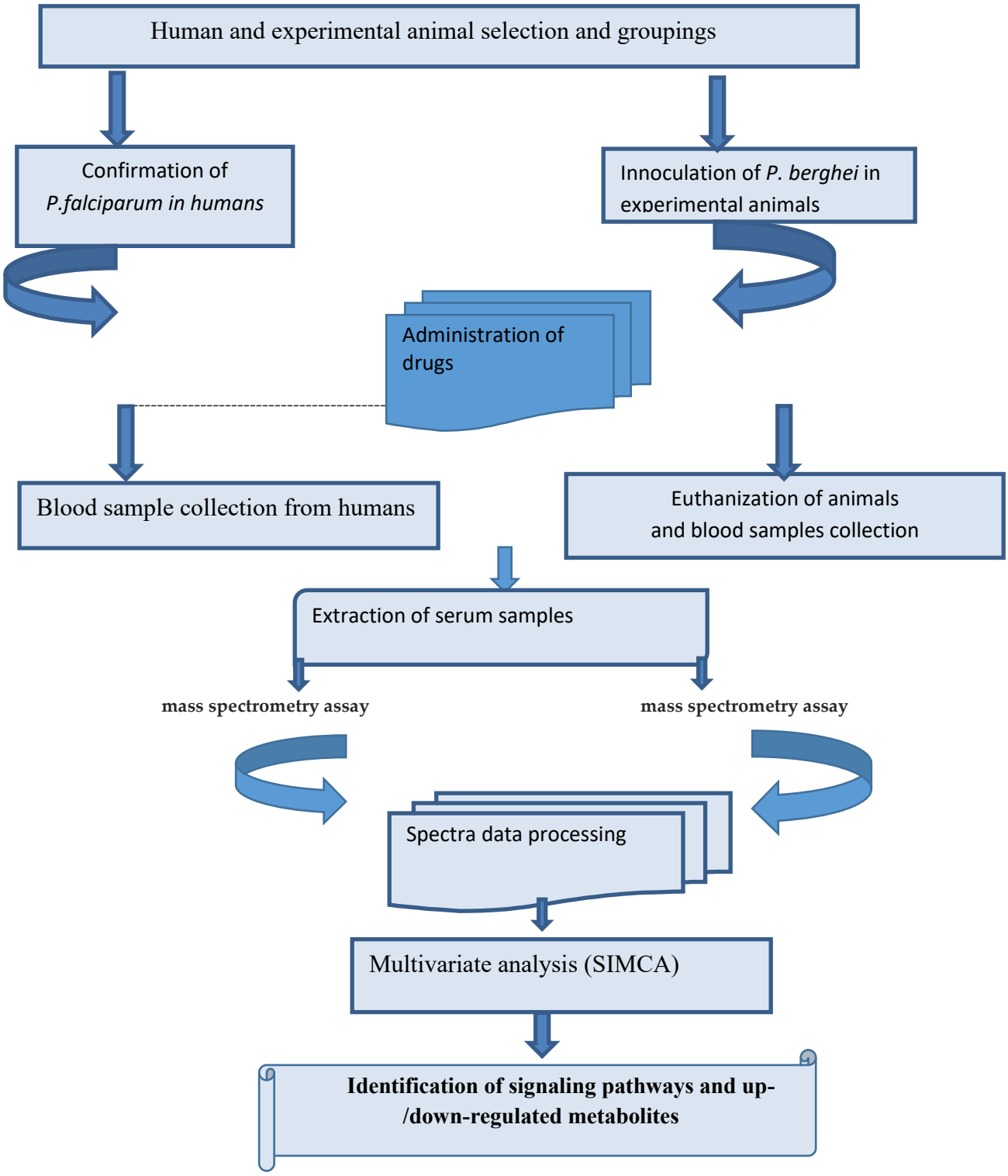

Figure 1. Flowchart depicting the steps adopted in the study

Peak detection in MZmine 2.12 was identified following noise removal, chromatogram construction, and peak deconvolution. In the first approach, the mass values were recorded using the centroid mode in each spectrum, and the peaks below 1×10^4 of the height were removed as noise. Chromatograms were noted for each of the mass values that spanned over a specific time range in the second step. The minimum time span over the same ion was programmed as 0.2 min and the error of the ion *m*/*z* value was allowed within 5 ppm.

The minimum intensity of the highest data point in the chromatogram was set at 1×10^4. Finally, a deconvolution algorithm was applied to each constructed chromatogram of each mass ion to recognize the actual chromatographic peaks. The "local minimum search" algorithm which searches for local minima in the chromatogram and the separated individual peaks at minimal points were used. The points of separating individual peaks were as follows: the chromatographic threshold at 95%; search minimum in RT range of 0.4 min; minimum relative height at 5%; minimum absolute height of 3×10^4; minimum ratio of peak top/edge three and peak duration range from 0.2 to 5.0 min. The separated peaks were then de-isotoped using the function of isotopic peaks grouper that was programmed at m/z tolerance at 0.001 m/z or 5.0 ppm; retention time tolerance at 0.1 absolute (min); maximum charge of 2; and a representative isotope that was most intensed. Retention time normalizer was also used after de-isotoping to reduce inter-batch variation by setting m/z tolerance at 0.001 m/z or 5.0 ppm; retention time tolerance at 0.5 absolute (min):and minimum standard intensity of 5.0×10^3. The remaining peaks in different samples were aligned based on the mass and retention time of each peak. The ion *m*/*z* tolerance for alignment was programmed at five ppm, retention time was five relative (%):and weight for *m*/*z* and Rt were 20 respectively. Following alignment, the resulting peak list was gap-filled with missing peaks using the intensity tolerance of 25% and retention time tolerance of 0.5 min. The solvent peaks were subtracted from the samples using peak intensity at a level above 1×10^5. The medium effects were then cleaned up using an Excel program which was written to subtract of medium peaks but remained features which were 20 times greater in the samples than in the medium. The data generated were then imported to SIMCA for further multivariate analysis (Macintyre *et al.*, 2014). MZmine with an in-house database was used. Reference identification of signaling pathways and up-/down-regulated significant metabolites were finally computed using the Human Metabolome Database (HMDB) and Kyoto Encyclopedia of Genes, and Genomes (KEGG) databases (Wishart *et al.*, 2007).

3. RESULTS

Metabolomic results of ACTs in experimental animals and humans

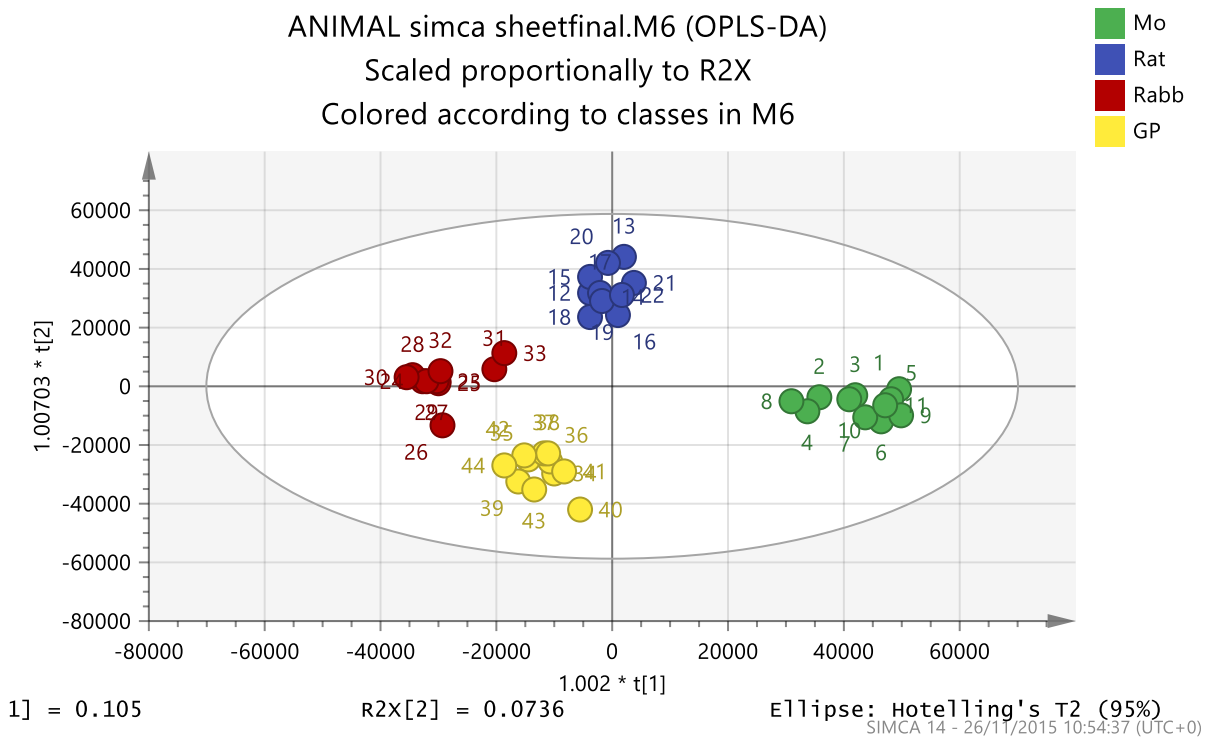

Figure 2: Orthogonal partial least squares-discriminant analysis (OPLS-DA) scatter plot of differentially separated metabolites of ACTs in experimental animals. The green colour represents mice, blue colour represents rats, brown colour represents rabbits, and yellow colour represents guinea pigs.MO: Mice, Rat: Rats, Rabb: Rabbits, GP: Guinea pigs.

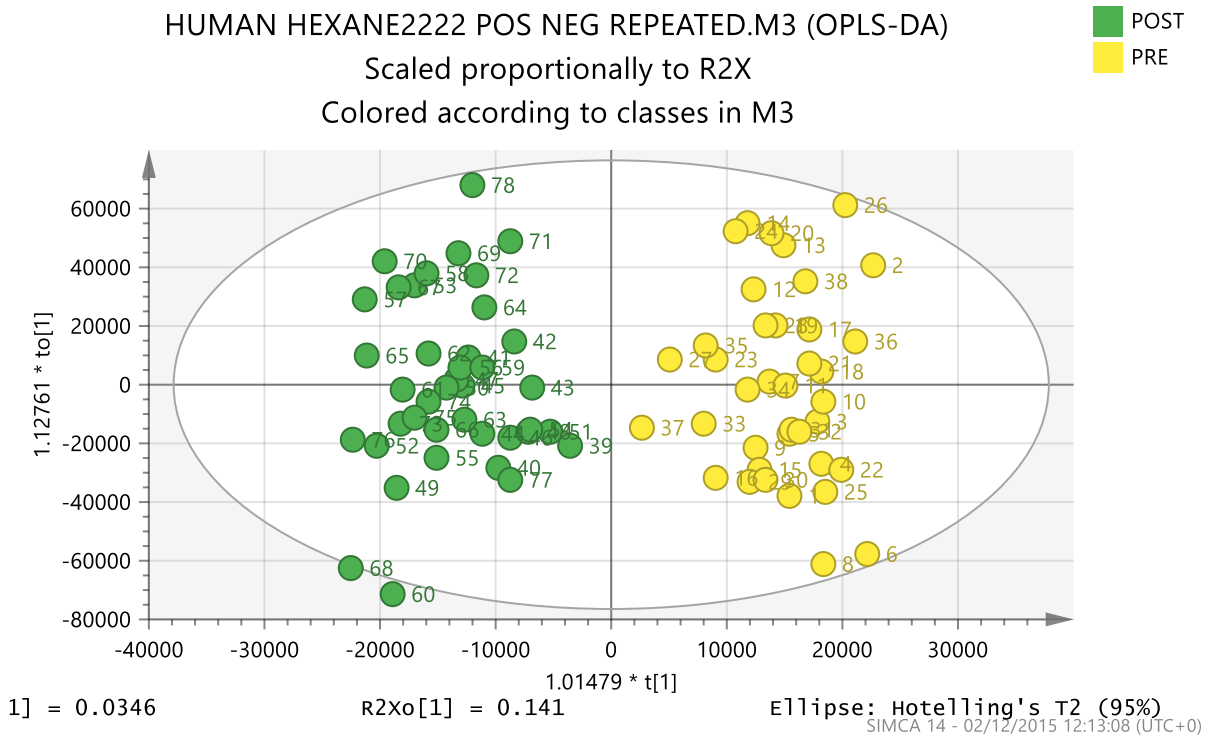

Figure 3: Orthogonal partial least squares-discriminant analysis (OPLS-DA) scatter plot of differentially separated metabolites of ACTs in human hexane extract. Samples between 1and 38 represent pre-drug administration and those that between 40 and 78 represent post-administration of ACTs. The yellow colour (PRE) represents pre-drug administration, the green colour (POST) represents post-drug administration.

Table 2. Summary of the significantly expressed metabolites and pathways due to ACTs (AL, AA, AM, ASP, DHP) in mice

ID	M/Z	*P*-value	MW	MF	Metabolite	Metabolic Pathway
100	896.77	-0.168	895.76	$C_5H_{104}O_9$	Tetradecanoyl-D-glycopyranosyl	Lipid
46	898.78	-0.166	897.78	$C_{52}H_{100}NO_8P$	Glycerophospholipid	Lipid
84	118.09	-0.142	117.08	$C_5H_{11}NO$	L-Valine	Amino-acid
3357	898.79	-0.996	898.78	$C_{52}H_{100}NO_8P$	Glycerophospholipid	Lipid
31	900.80	-0.115	899.79	$C_{52}H_{102}NO_8P$	Glycerophospholipid	Lipid
286	900.80	-0.100	899.79	$C_{52}H_{102}NO_8$	Glycerophospholipid	Lipid
26	178.06	-0.272	180.64	$C_6H_{12}O_6$	D-glucose	Carbohydrate
195	159.11	-0.084	158.11	$C_7H_{14}N_2O_2$	Valine	Amino acid
2224	391.29	-0.098	392.293	$C_{24}H_{40}O_4$	Dihydroxy-cholanoic acid	Lipid
3354	872.77	-0.102	871.703	$C_{50}H_{98}NO_8P$	Octadecanoyl-glycerol	Lipid
1	281.25	0.141	282.26	$C_{18}H_{34}O_2$	Tetradecanoic acid	Lipid
69	234.08	0.12	233.87	$C_3H_6S_6$	Hexathionane	Lipid
11	132.08	0.117	131.069	$C_4H_9N_3O_2$	Creatine	Amino acid
66	311.08	0.114	310.07	$C_{12}H_{14}N_4O_4S$	Sulphadoxine	Xenobiotic
6	162.11	0.110	161.105	$C_7H_{15}NO_3$	Carnitine	Amino acid
2677	311.08	0.110	310.07	$C_{12}H_{14}N_4O_4S$	Sulphadoxine	Xenobiotic
3	279	0.103	280.24	$C_{18}H_{32}O_2$	9,5-Octadeca-dienoic	Lipid

					acid	
10	204.12	0.09	203.12	$C_9H_{17}NO_4$	Glutamic acid	Amino acid
752	104.11	0.09	103.10	C_4H_9NO	4-aminobutanoate	Amino acid
223	247.08		248.08287	$C_{12}H_{13}N_4Cl$	Pyrimethamine	Xenobiotics Drugs

Abbreviations: ID: Identification number, M/Z: Mass to charge ratio, MW: Molecular weight, MF: Molecular formula, ACTs: Artemisinin-Based Combination Therapies, AL: Artemether-Lumefantrine, AA: Artesunate-Amodiaquine, AM: Artesunate-Mefloquine, ASP: Artesunate-Sulphadoxine-Pyrimethamine, and DHP: Dihydroartemisinin-Piperaquine.

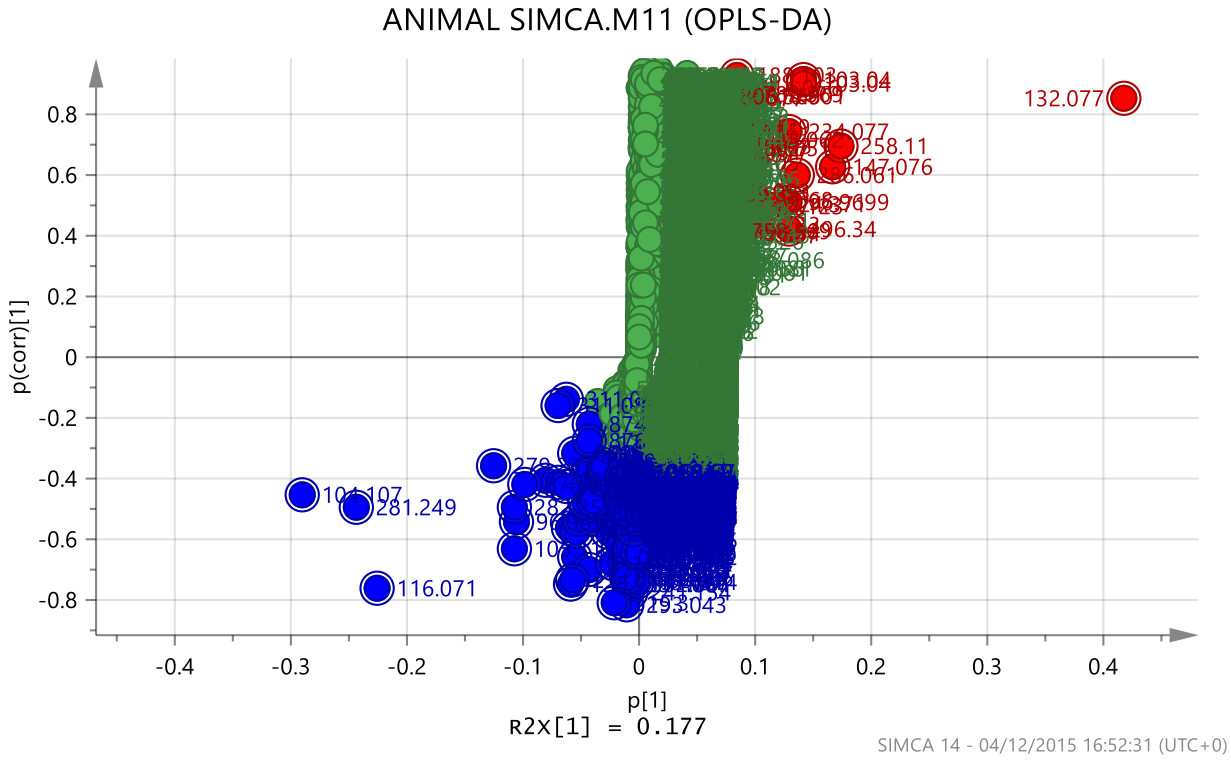

Figure 4: OPLS-DA S-plots of hexane as non-polar samples in mice. The significantly down-regulated metabolites represent blue colour while the significantly up-regulated metabolites represent the red colour.

Table 3: Summary of the significantly expressed metabolites and pathways due to ACTs (AL, AA, AM, ASP, DHP) in Rabbits

ID	M/Z	*P*-value	MW	MF	Metabolite	Metabolic Pathway
62	172.91	-0.07	228.21	$C_{14}H_{28}O_2$	Tetradecanoic acid	Lipid
1066	234.077	-0.047	233.07	$C_{12}H_{11}NO_4$	Hexa-2,4-dienoate	Lipid
1712	255.23	-0.037	256.24	$C_{16}H_{32}O_2$	Hexadecanoic acid	Lipid
507	173.96	-0.022	174.97	$C_4H_2BrNO_2$	Pyrrole-2,5-dione	Amino acid
253	279.16	-0.028	278.15	$C_{16}H_{22}O_4$	2-ethylhexyl-phthalate	Amino acid
796	445.17	-0.092	444.16	$C_{20}H_{24}N_6$	Trp-Cys-His	Amino acid
331	91.05	-0.071	92.05	$C_3H_8O_3$	Glycerol	Carbohydrate
61	84.14	-0.013	86.08	$C_4H_{10}N_2$	Piperazine	Xenobiotics Drugs
841	87.12	-0.001	88.02	$C_3H_4O_3$	Pyruvate	Carbohydrate
856	103.04	-0.193	104.04	$C_4H_8O_3$	Hydroxybutanoate	Lipid
29	114.06	0.230	113.06	$C_4H_7N_{30}$	Creatinine	Amino acid
753	116.07	0.65	116.07	$C_6H_{12}O_2$	Hexadecanoic acid	Lipid
7	147.08	0.18	146.07	$C_6H_{10}O_4$	Adipate	Lipid

3	118.09	0.16	117.07	$C_5H_{11}NO_2$	L-valine	Amino acid
4	496.34	0.16	495.33	$C_{24}H_{50}NO_7P$	Hexadecaoyl-glycero-3-phosphocholine	Lipid
30	279.23	0.15	280.24	$C_{18}H_{32}O_2$	Linoleic acid	Lipid
21	758.57	0.146	757.56	$C_{42}H_{80}NO_8P$	Octadecadienoyl-glycerol	Lipid
1	281.25	0.141	282.26	$C_{18}H_{34}O_2$	Artemisinin	Xenobiotic
451	102.12	0.11	103.06	$C_4H_9NO_2$	4-Aminobutanoate	Amino Acid
108	101.02	0.13	102.03	$C_4H_6O_3$	2-Oxobutanoate	Amino Acid

Abbreviations: ID: Identification number, M/Z: Mass to charge ratio, MW: Molecular weight, MF: Molecular formula, ACTs: Artemisinin-Based Combination Therapies, AL: Artemether-Lumefantrine, AA: Artesunate-Amodiaquine, AM: Artesunate-Mefloquine, ASP: Artesunate-Sulphadoxine-Pyrimethamine, and DHP: Dihydroartemisinin-Piperaquine.

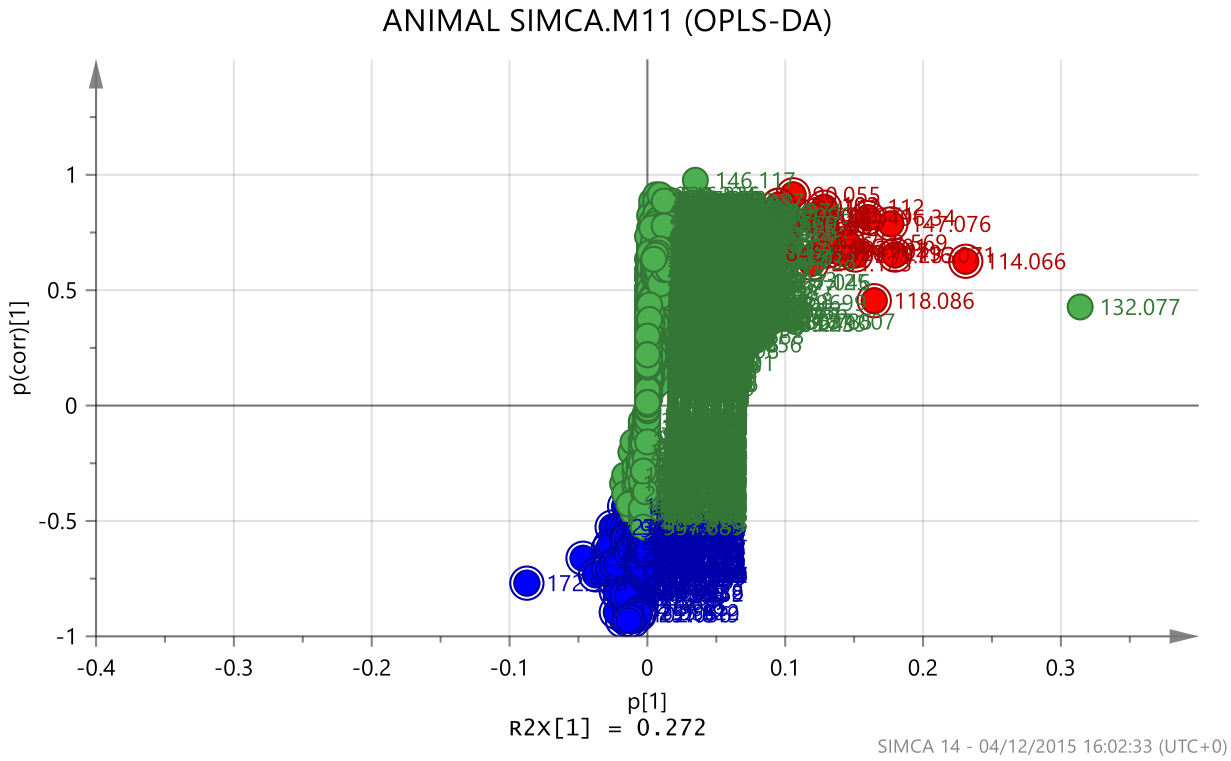

Figure 5: OPLS-DA S-plots of hexane as non-polar samples in Rabbits. The significantly down-regulated metabolites represent blue colour while the significantly up-regulated metabolites represent red colour.

Table 4. Summary of the significantly expressed metabolites and pathways due to ACTs (AL, AA, AM, ASP, DHP) in Guinea pigs

ID	M/Z	*P*-value	MW	MF	Metabolite	Metabolic Pathway
100	895.76	-0.108	896.77	$C_{52}H_{98}NO_8P$	Glycero-phosphocholine	Lipid
46	897.78	-0.106	898.78	$C_{46}H_{76}O_{13}P_2$	Glycero-phosphocholine	Lipid
3357	897.78	-0.106	898.78	$C_{46}H_{76}O_{13}P_2$	Glycero-phosphocholine	Lipid
3	117.08	-0.142	118.09	$C_5H_{11}NO_2$	L-valine	Amino acid
31	899.79	-0.111	900.80	$C_{52}H_{102}NO_8P$	Glycero-phosphocholine	Lipid
3354	871.76	-0.102	872	$C_{50}H_{98}NO_8P$	Glycero-phosphocholine	Lipid
2224	392.29	-0.098	391.286	$C_{24}H_{40}O_4$	Dihydroxy Cholan-24-oic acid	Lipid
286	899.79	-0.100	900.80	$C_{52}H_{102}NO_8P$	Glycero-phosphocholine	Lipid

1489	895.76	-0.093	896	$C_{52}H_{96}NO_8P$	Glycero-phosphocholine	Lipid
1	282.26	0.141	281.25	$C_{18}H_{34}O_2$	Artemisinin	Xenobiotic
69	233.07	0.12	234.08	$C_{12}H_{11}NO_4$	Hexa-2,4-dienoate	Lipid
11	131.076	0.12	132.08	$C_4H_9N_3O_2$	Creatine	Amino acid
66	310.07	0.11	311.08	$C_{12}H_{14}N_4O_4S$	Sulphadoxine	Xenobiotic
2677	310.07	0.11	311.08	$C_{12}H_{14}N_4O_4S$	Sulphadoxine	Xenobiotic
6	161.05	0.11	162.11	$C_7H_{15}NO_3$	L-Carnitine	Amino acid
3	280.24	0.10	280.24	$C_{18}H_{32}O_2$	Octadecanoic acid	Lipid met
10	203.11	0.09	204.12	$C_9H_{18}NO_4$	O-Acetylcarnitine	Amino acid
752	103.10	0.09	104.107	$C_4H_9NO_2$	N- Butanoate	Amino acid
417	92.05	0.007	91.03	$C_3H_8O_3$	Glycerol	Carbohydrate
74	89.05	0.12	88.31	$C_3H_7NO_2$	L-Alanine	Amino Acid
2296	86.084	0.11	85.074	$C_4H_{10}N_2$	Piperazine	Xenobiotics
241	88.02	0.19	87.04	$C_3H_4O_3$	Pyruvate	Carbohydrate

Abbreviations: ID: Identification number, M/Z: Mass to charge ratio, MW: Molecular weight, MF: Molecular formula, ACTs: Artemisinin-Based Combination Therapies, AL: Artemether-Lumefantrine, AA: Artesunate-Amodiaquine, AM: Artesunate-Mefloquine, ASP: Artesunate-Sulphadoxine-Pyrimethamine, and DHP: Dihydroartemisinin-Piperaquine.

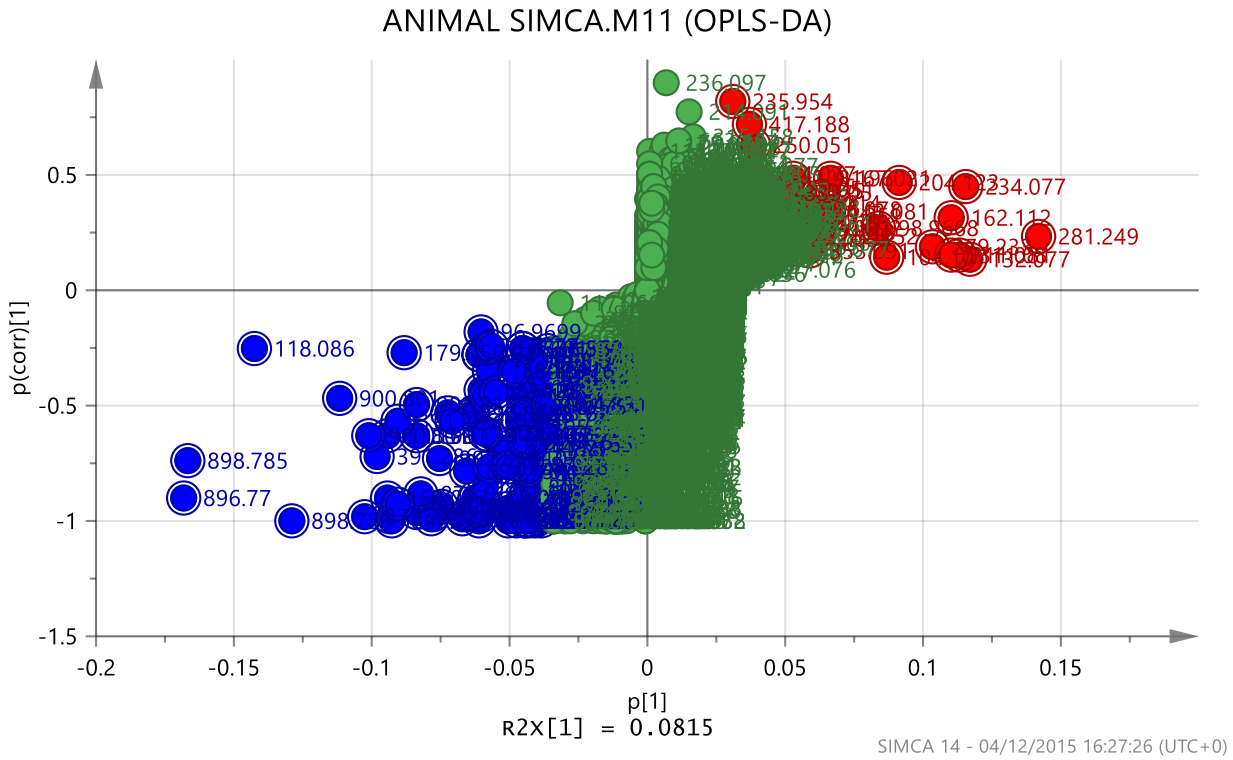

Figure 6: OPLS-DA S-plots of hexane as non-polar samples in Guinea pigs. The significantly down-regulated metabolites represent blue colour while the significantly up-regulated metabolites are represent red colour.

Table 5. Summary of the significantly expressed metabolites and pathways due to ACTs (AL, AA, AM ASP, DHP) in Rats

ID	M/Z	*P*-value	MW	MF	Metabolites	Metabolic Pathway
28	875.79	-0.66	876.80	$C_{51}H_{90}NO_8P$	Glycerophospholipid	Lipid
62	130.06	-0.01	131.04	$C_6H_{10}O_3$	Oxopentanoic acid	Lipid
10	99.97	-0.07	98.97	H_3O_4P	Orthophosphate	Energy
752	104.11	-0.08	104.11	$C_4H_9NO_2$	4-aminobutanoate	Amino acid

66	310.07	-0.07	311.08	$C_{12}H_{14}N_4O_4S$	Sulphadoxine	Xenobiotic drug
3	117.08	-0.06	118.09	$C_5H_{11}NO_2$	L-valine	Amino acid
1	282.26	-0.04	281.25	$C_{15}H_{22}O_5$	Artemisinin	Xenobiotic drug
2097	211.09	-0.04	212.09	$C_{10}H_{13}N_20_4$	Methoxy-tyrosine	Amino acid
1652	195.05	-0.04	195.05	$C_{10}H_{13}N0_3$	L-tyrosine ester	Amino acid
519	455.86	-0.01	484.85	$C_{27}H_{53}NO_4$	Arachidyl-carnitine	Amino acid
6	161.11	0.22	162.11	$C_7H_{15}NO_3$	L-carnitine	Amino acid
2338	142.07	0.19	143.08	$C_6H_{10}N_2O_2$	Ectoine	Amino acid
10	203.12	0.16	204.12	$C_9H_{18}NO_4$	O-acetyl carnitine	Amino acid
753	115.06	0.14	114.08	$C_5H_{10}N_2O$	L-proline amide	Amino Acid
7	146.07	0.13	147.08	$C_6H_{10}O_4$	Adipate	Lipid
9	134.02	0.14	133.01	$C_4H_6O_5$	S-malate	Citrate cycle
1	131.07	0.12	132.08	$C_4H_9N_3O_2$	Creatine	Amino acid
21	757.56	0.12	758.57	$C_{42}H_{80}NO_8P$	Glycerophosphocholine	Lipid
6	125.02	0.12	124.01	$C_2H_7NO_3S$	Taurine	Lipid
102	193.07	0.11	192.02	$C_{10}H_{11}NO_3$	Phenylacetylglycine	Amino Acid

Abbreviations: ID: Identification number, M/Z: Mass to charge ratio, MW: Molecular weight, MF: Molecular formula, ACTs: Artemisinin-Based Combination Therapies, AL: Artemether-Lumefantrine, AA: Artesunate-Amodiaquine, AM: Artesunate-Mefloquine, ASP: Artesunate-Sulphadoxine-Pyrimethamine, and DHP: Dihydroartemisinin-Piperaquine.

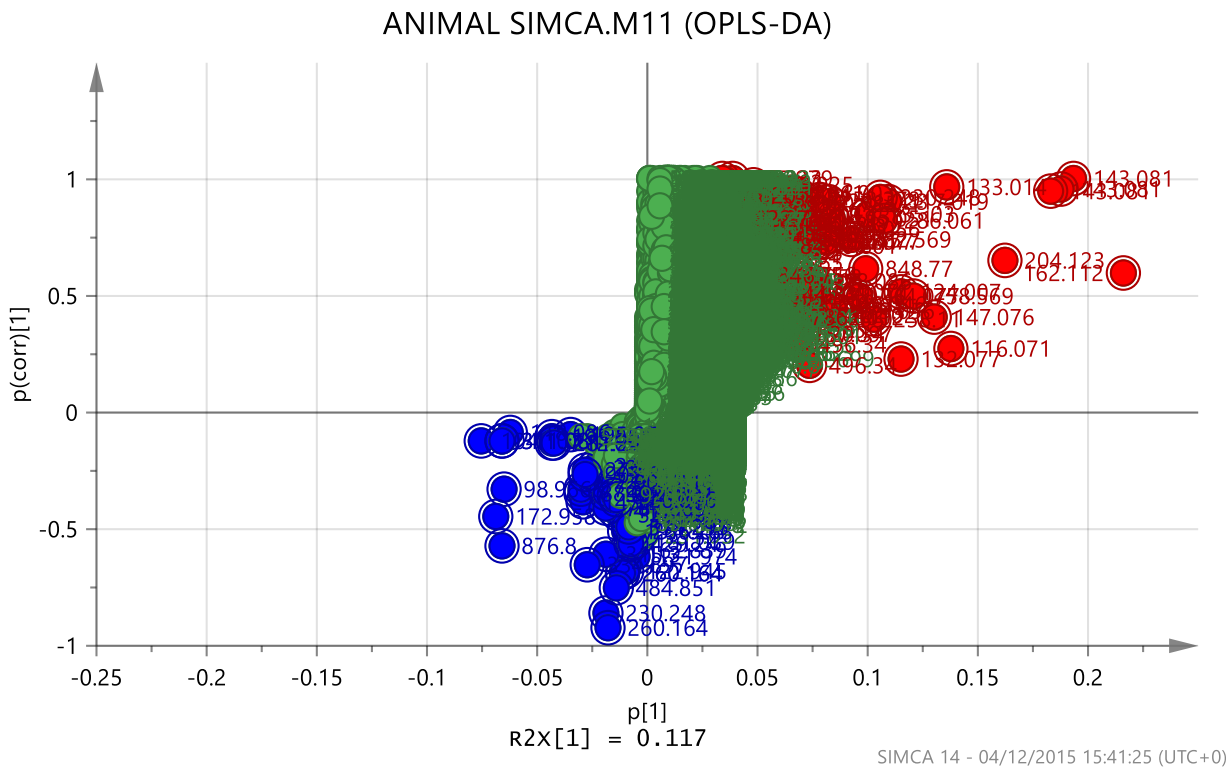

Figure 7: OPLS-DA S-plots of hexane as non-polar samples in rats. The significantly down-regulated metabolites represent blue colour while the significantly up-regulated metabolites represent red colour.

Table 6. Summary of the significantly expressed metabolites and pathways due to ACTs (AL, AA, AM, ASP, DHP) in humans

ID	M/Z	*P*-value	MW	MF	Metabolite	Metabolic Pathway
98	179.06	-0.12	180.06	$C_6H_{12}O_6$	D-Glucose	Carbohydrate
3004	193.11	-0.21	192.11	$C_{12}H_{16}O_2$	Tetraenoic acid	Lipid
4898	255.23	-0.09	256.24	$C_{16}H_{32}O_2$	Hexadecanoic acid	Lipid
5585	283.27	-0.09	284.20	$C_{18}H_{36}O_2$	Ocatadecanoic acid	Lipid

2182	162.11	-0.08	161.11	$C_7H_{15}NO_3$	L-carnitine	Amino acid
568	103.10	-0.08	130.10	$C_5H_{13}NO$	Choline	Amino acid
547	104.07	-0.08	103.10	$C_4H_9NO_2$	4-Aminobutanoate	Amino acid
1257	129.07	-0.06	128.06	$C_5H_8N_2O_2$	5,6-Dihydrothymine	Amino acid
2227	164.07	-0.05	163.06	$C_6H_{13}NO_2S$	Cysteine	Amino acid
2221	164.07	-0.04	163.06	$C_4H_9N_3O_4$	Amino-alanine	Amino acid
3088	194.08	-0.03	195.09	$C_{10}H_{13}NO_3$	L-tyrosine methyl ester	Amino acid
84	84.01	0.17	85.01	$C_5H_{11}N$	Piperidine	Piperidine
1496	136.05	0.12	136.05	$C_8H_8O_2$	Phenylacetic acid	Amino acid
337	94.98	0.11	95.99	CH_4O_3S	Methane sulphonic acid	Sulphonic acid
756	387.18	0.07	387.18	$C_{15}H_{26}N_2O_4S$	Peptide: Lys-Cys-His	Amino acid
4908	255.23	0.07	256.24	$C_{16}H_{32}O_2$	Hexadecanoic acid	Lipid
112	173.06	0.04	174.10	$C_{12}H_{14}O$	Dodecapentaenal	Lipids
915	229.10	0.16	230.19	$C_{13}H_{26}O_3$	Tridecanoic acid	Lipid
86	758.57	0.15	759.58	$C_{42}H_{82}NO_8P$	Glycero-phosphocholine	Lipid
119	143.04	0.12	144.04	$C_6H_8O_4$	2,3-Dimethylmaleate	Cofactors
532	145.05	0.01	146.06	$C_6H_{10}O_4$	Adipate	Lipid
67	806.57	0.42	805.56	$C_{46}H_{80}NO_8P$	Glycero-phosphocholine	Lipid
7	165.04	0.01	166.05	$C_5H_{10}O_6$	L-Arabinonate	Carbohydrate

Abbreviations: ID: Identification number, M/Z: Mass to charge ratio, MW: Molecular weight, MF: Molecular formula, ACTs: Artemisinin-Based Combination Therapies, AL: Artemether-Lumefantrine, AA: Artesunate-Amodiaquine, AM: Artesunate-Mefloquine, ASP: Artesunate-Sulphadoxine-Pyrimethamine, and DHP: Dihydroartemisinin-Piperaquine.

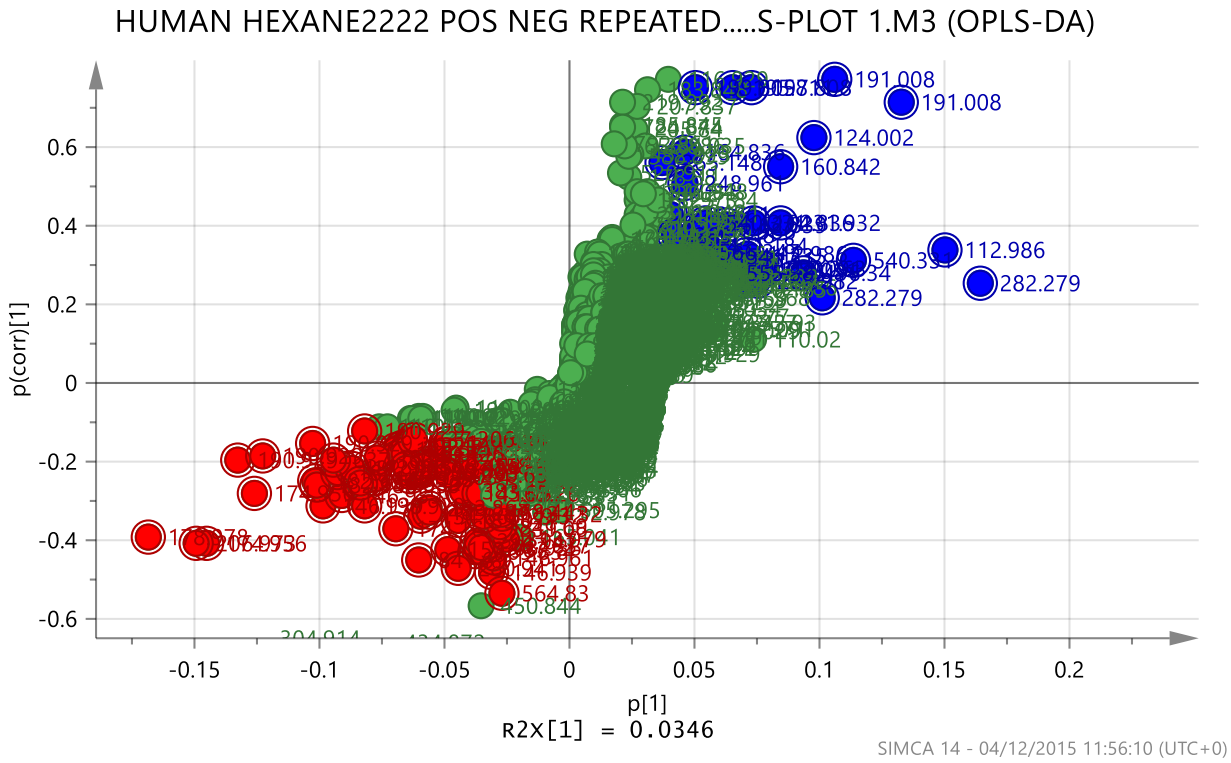

Figure 8: OPLS-DA S-plots of hexane as non-polar samples in humans. The significantly down-regulated metabolites represent red colour while the significantly up-regulated metabolites represent blue colour.

Table 7: Outlier Analysis

ANIMALS	(N)	R^2X	R^2Y	Q^2Y
Mice (Control group Vs Test group)	44	0.18	0.79	0.27
Rats (Control group Vs Test group)	44	0.92	1	0.77
Rabbits (Control group Vs Test group)	44	0.27	0.54	-0.14
Guinea Pigs (Control group Vs Test group)	44	0.75	1	0.57
HUMANES (PreVs Post-drug admin)	78	0.37	0.98	0.72

Correlation and prediction (R^2X/R^2Y, Q^2Y) between control groups and test groups for mice, rats, rabbits, and guinea pigs. The correlation and prediction (R^2X/R^2Y, Q^2Y) between Pre-drug administration and post-drug administration for humans. N: Total number of samples.

4. DISCUSSION

The results showed metabolomic differences in experimental animals and humans due to commonly used ACTs as in Figures 2 and 3. Patients who reported with uncomplicated malaria due to *P. falciparum* infection showed similar alteration of metabolites compared to the animal models infected with *P.berghei*. It has been reported that the human body contain approximately 3000 to 5000 detectable metabolites, a sizable fraction has been identified (Wishart *et al.,* 2007). In the pool of findings, D-glucose, creatinine, glutamate, aspartate, glycine, taurine, eicosapentaeinoyl-glycerol, hexadecanoic acid, amino-butanoate, and L-tyrosine were the significantly altered metabolites as in Tables 2 to 6. In contrast lipids, amino acid, carbohydrate, and nucleotide were the significantly altered pathways (OPLS-DA). Meanwhile, all these common metabolites and pathways have been identified in the *P. falciparum* genome (Gardner *et al*., 2002). The differences in metabolites and metabolic pathways as seen in this study could be due to interference by ACTs as in Tables 2 to 6. These differences in the expression of metabolites as in Figures 2 to 8 could also be linked to the confirmed *Plasmodium falciparum* in humans or the inoculated *Plasmodium berghei* in the experimental animals. These factors could also be influenced by diet, age, gut microflora, xenobiotics, and severity of diseases as reported (Nicholson, 1999). The effects may also be dose-dependent and the sensitivity of infection irrespective of the ACTs. These phenomena support the report that smaller models like mice are more dose sensitive and may present with more toxicities than humans (Aghahowa *et al.,* 2021). The metabolic derangement seen in the expression of metabolites as in Tables 2 to 6, may not have occurred until there was a significant interference with the metabolites in the tissue or organ by the ACTs. There may have been minor changes before exposure as seen in pre-drug administration in human and the control groups in animals. The wide array of metabolic expression in Figures 4 to 8. can be associated with the different toxicity pattern and inherent mechanism of action of ACTs interfering with the endogenous molecules, such as carbohydrates, amino acids, nucleotides, phospholipids, fatty acids, and their derivatives. The organs (Nicholson, 1999) and the cells (Gardner *et al*., 2002) may also represent the unit of target. Since there were metabolic changes in the biologic system of the models, it represents an insight in the interference with the biochemical pathways giving rise to the changes observed in Figures 2,3,4,5,6. Significant disturbances in several metabolic pathways, as observed in this study are similar to those reported (Zhang *et al*., 2008):where amino acid, lipid, and nucleotide pathways, have been altered, leading to the up-regulation/down-regulation of different metabolites. Specie metabolomic difference in the animals and humans can be interpreted as the differences in the rate and extent of absorption, type of metabolic detoxification of ACTs in the liver. Other metabolites altered, have been proposed to be different in the species of animals due to drug insults (Nicholson *et al*., 2012). These differences might explain the variable toxicity of ACTs between strains in terms of the metabolic fate and receptor densities. The potential toxicity of the drugs investigated can be associated with the activity in the alteration of different endogenous pathways (Nicholson *et al*., 2012). The difference observed may be due to ACTs showing several alterations which may not be whole or section organ specific as previously reported (Nicholson *et al*., 2012). Xenobiotic such as sulphadoxine, pyrimethamine, artemisinin were up-regulated commonly in all the models. These xenobiotics have validated the type of ACTs administered in Table 1, and also represent the potential metabolites that could cause toxicity. This annotated information strengthens the fate of ACTs toxicities in animals and humans that were identified in the class of xenobiotics (Zimmerman, 1999): that may be potentially toxic in the models. These results also suggest a similar enzymatic activity of ACTs in the liver as reported in a past study (Aghahowa *et al*., 2021).

The contributory effects of parasites present remain an influential tool that can lead to the up-regulation of metabolites identified. It is interesting to note that a specific metabolite has been reported in specific pathways in microbial infection (Gardner *et al*., 2002; Li *et al*., 2013). During the course of the study, malaria infection was simulated by inoculating *P. berghei* in all the animals before drug administration. Also, the confirmed *P. falciparum* organism during recruitment of participants before drug administration buttresses the identification of different metabolites in patients recruited. This research therefore, calls for further investigation in order to

differentiate intra-/inter- specie metabolomic variation in all the models in a typical malaria condition. Specific metabolites that span through carbohydrates, lipids, and amino acids identified in this study have been documented as specific markers of the plasmodial organism (Gardner *et al*., 2002). The use of *P. berghei* in the experimental animals may have shown a clear difference in humans who had *P. falciparum* in the metabolomic phenomena. Meanwhile, it has been documented in past reports that the rat model of malaria resembles that of human malaria symptoms, such as hyper-parasitaemia and lethality, but still they differ in the pathogenesis when compared to mice (Xie *et al*., 2006). These similarities and differences may be linked to the expression of the related and unrelated metabolites that were observed. It has been reported that there might be host-protozoa interactions (Li *et al*., 2013). These can also be noted as drug-protozoa interactions, which may have taken place between the expressed metabolite and the inherent biochemical components of the organism (Li *et al*., 2013): that may have influenced some of the results seen in this study. However, interaction between parasites and endogenous components of the host has been reported to be involved in the puritogenic effect of some anti-malarials (Aghahowa *et al*., 2010). Differences in the pathogenesis of *Plasmodia* organisms have been reported in different rodents and other animal models (Krettli *et al*., 2009). Mice are most susceptible, and also known to develop acute fulminating disease induced by blood stage parasites, or by sporozoites injected either through mosquito bite or intravenously. Rats have been identified to develop chronic malaria disease and live for long periods and they may cure the infection spontaneously (Krettli *et al*., 2009). However, metabonomic analysis of *P. falciparum*-infected erythrocytes performed using LC-MS, showed that the metabolites were altered by the developmental cycle of the parasite. Some of the metabolites and metabolic pathways identified in this study support the unit target in the *Plasmodium falciparum* genome (Gardner *et al*., 2002) as the basis for understanding the possible mechanisms of action of ACTs in Table 1. The depletion of arginine caused by the parasite may be associated with cerebral malaria pathogenesis in human (Olszewski *et al*., 2009). Alterations in the TCA cycle with *P. falciparum* infection were noted in another investigation where over 150 differentially annotated metabolites were found, and additional changes, such as the urea cycle, and metabolism of nucleotide, amino acid, sphingolipid and fatty acid have been reported (Sana *et al*., 2013). Interestingly, the contributory effect of plasmodial organisms had produced over 10,000 unique metabolic moities, a number that is indicative of the complexity of the human metabolome and the potential target in metabolomics in biomarker discovery (Want *et al*., 2006). The metabolic profile of a biofluid could allow for the prediction of toxicity and the detection of diseases (Want *et al*., 2006). These biofluids have been reported to contain many metabolites. The human metabolome is estimated to contain 7,800 metabolites, not including many metabolites related to gut microflora, lipid and drug metabolism (Dun *et al*., 2011). This may provide an appropriate reliability of the potential effects of ACTs on human body. Malaria patients being a higher model that participated in the study may justify the increase and varied number of metabolites compared to the experimental animals due to ACTs. Research has shown that cerebral malaria in the *P. berghei* mouse model was shown to have decreased levels of phosphocreatine, glutamate, γ-aminobutyric acid, and alanine, accompanied by increased levels of glutamine in the brain (Parekh *et al*., 2006). Therefore, the expression of pyruvate, glucose, creatine, and glycerophosphorylcholine as similar analogues (Parekh *et al*., 2006) of reported metabolites may be shown in cerebral malaria. All these strongly suggest that the expressed metabolites are potential tools in identifying malaria features. The reports of similar metabolites such as lactate, pyruvate, citrate, acetate, creatine, glycerophosphorylcholine, glucose and choline in mouse plasma infected with *P. berghei* (Parekh *et al*., 2006) are further confirmation in the biofluid composition in this study. Cellular differences are found in cells of erythrocytes with *P. falciparum*, which also contain metabolites such as α-ketoglutarate, lactate, 5-methylthioinosine, thymidine, allantoate, malate, aconitate, citrate, ornithine, and urea (Olszewski *et al*., 2009): thus, showing differences in metabolic pathways due to the species of Plasmodium. These variations suggest another line of research using different plasmodia species in animal models to check the effects of different ACTs. The elevation of fatty acids reflects the effect ACTs might have had in the phospholipid arachidonic acid pathway (Rang *et al*., 2012): thus, regulating the production of prostaglandins and thromboxanes that might be associated in pain and body weakness commonly reported due to ACTs (Bassi *et al*., 2013; Aghahowa *et al*., 2014; Aghahowa *et al*., 2021). This may also emphasize the mechanism of action of ACTs in Table 1, as seen in the interference with various pathways.

In this study, hierarchical clustering was performed to highlight similarities in the metabolite features observed between the mice, rats, guinea pigs, rabbits, and humans in Figures 2 and 3. This S-plot (OPLS-DA) showed up-regulation/down-regulation of unique metabolites in the various models. These interferences with metabolites such as aspartate, glutamate, glycine, taurine, and phospholipids could help in better understanding of the pharmacological activities of ACTs. The observed increase in the glutamine concentration can alter the neuronal-glial glutamate-glutamine cycling, which may result in an increased glucose concentration (Rang *et al*., 2012). Also, the up-regulation of succinic acid concentration might be due to the inhibition of succinate dehydrogenase, an enzyme linked that is to the mitochondrial respiratory chain and TCA cycle (Rang *et al*., 2012; Sana *et al*., 2013). Glutamic acid has been reported

as a precursor in the synthesis of catecholamines (Rang *et al.,* 2012) thus suggesting catecholamine activity could be altered by ACTs in some patients during therapy. In addition, the observed difference in lactate supports a deficiency of oxidative energy metabolism. Therefore, the observed difference in glucose must have been caused by a perturbation in another metabolic pathway that may cause hypoglycemia or hyperglycemia that may be familiar with some ACTs (Falade and Manyando, 2009; Aghahowa *et al.,* 2014; Aghahowa *et al.,* 2021). The observed increase in glutamine is a reflection of decreased glutaminase activity. Glutaminase is a mitochondrial enzyme (Tsang *et al.,* 2006) found in neurons that takes care of the conversion of glutamine to glutamate. Perturbation of the glutamate–glutamine cycling may indicate an impairment of energy metabolism and mitochondrial respiration (Tsang *et al.,* 2006) that are essential in physiological processes. Thus, a decrease in glutaminase activity precludes the conversion of glutamine into glutamate. Owing to this, the study suggests that ACTs may affect glutamate transmission that may ultimately produce an upsurge pharmacological effects. The up-regulated succinic acid due to ACTs in some of the models may be due to the inhibition of succinate dehydrogenase (Rang *et al.,* 2012): as an essential enzyme in the mitochondria of cells. This enzyme is known to support the oxidation of succinic acid to fumarate in the tricarboxylic acid (TCA) cycle (Rang *et al.,* 2012). Most metabolites such as acylcarnitines, amino acids, biogenic amines, glycerophospholipids, sphingolipids, and hexose observed in this study are in line with previously identified metabolites in serum and plasma in population-based studies (Floegel *et al.,* 2011). Other metabolite such as creatinine has been reported. This metabolite is not only common as a kidney biomarker, but can be found in plasma and serum in varied concentration (Everett, 2015):as an indicator of oxidative stress in kidney damage. The up-regulation/down-regulation of amino acids and related metabolites can be linked to the wide range of amino acids that may go into the TCA cycle to produce urea. Some of these amino acids are precursors for the synthesis of serotonin and catecholamines (Rang *et al.,* 2012; Everett, 2015). The metabolomic interference of ACTs with precursors such as tyrosine in the synthesis of catecholamines (Rang *et al.,* 2012): showed that the combination therapies has a key role in the alteration of the endogenous transmitters that may finally alter cardiovascular events reported in some individuals using ACTs (Aghahowa *et al.,* 2014). Therefore, caution needs to be taken because up-regulation of some metabolites as observed in the study can lead to upsurge that may further lead to fatal systemic effects of some unpredictable transmitters that may be implicated in reported toxicities (Aghahowa *et al.,* 2021). The main objective of glycolysis is to provide energy for the cell, but there is increasing evidence that glycolysis is likely an adaptation to hypoxic conditions (Gardner *et al.,* 2002; Beger, 2006). Once there is an alteration of glucose, pyruvate, and other energy linked metabolites; this can induce stress in the pathway thus initiating stress signaling in the cell that will generate a pool of reactive species to induce oxidative stress. This may be the consequence of documented adverse effects reported in ACTs (Bassi *et al*., 2013; Aghahowa *et al.,* 2014; Aghahowa *et al.,* 2021).

The metabolomic phenomena of ACTs may not only be linked to toxicity alone, but they can also be ascribed to resistance. There may be metabolites expressed that can aid in the synthesis of folate, that can aid in microbial survival (McCarthy *et al.,* 2011). The presence of metabolites such as glutamic acid which act as a precursor in folic acid structural framework, can act as a moiety in the biochemical pathway in the synthesis of the folic acid (Gardner *et al.,* 2002; Rang *et al.,* 2012): thus, leading to parasite survival. This mechanism can confer resistance in plasmodia organisms in some patients who may report with failures during therapy (McCarthy *et al.,* 2011; Rang *et al.,*2012). Glycine is also an essential precursor in purine synthesis (Rang *et al.,* 2012). This can form a ligand with succinyl-CoA in the synthesis of heme (McCarthy *et al.,* 2011; Rang *et al.,* 2012; Cheng *et al.,* 2015): which may also account for parasite survival. Metabolomic predictivity and reliability in the order safety of ACTs in Table 7, had further buttressed the adoption of ACTs in health policies and researches carried out independently using traditional toxicity markers (WHO, 2001; FMOH, 2005; Bassi *et al.,* 2013; Aghahowa *et al.,* 2021). Interestingly, the findings in the order of safety in Table 7, is in concordance with a previous report (Aghahowa *et al.,* 2021). In all, this science of metabolomic research has demystified the complexities of efficacy, toxicity, and resistance due to ACTs. Large scale independent studies in different regions are recommended to support the findings.

4. CONCLUSION

The study has shown the pattern of metabolomic alteration of the endogenous metabolites and pathways in mice, rats, rabbits, guinea pigs, and humans due to Artemisinin-Based Combination Therapies. The reports in this study, therefore provide mechanistic phenomena in understanding the efficacy and toxicity of ACTs in malaria therapy. In the forgoing, the annotated metabolomic studies can be a valuable template in the selection of recommended ACTs in malaria therapies and researches.

Acknowledgements
We wish to acknowledge all staff and students of the Department of Pharmacology and Toxicology, University of Benin, Nigeria for their immerse contribution. Special thanks go to Dr Ru-angelie Edrada-Ebel, Tong Zhang and other members of metabolomic group that supervised the work and did the simca analysis/dereplication respectively in the Strathclyde Institute of Pharmacy and Biomedical Science, University of Strathclyde Glasgow, United Kingdom. The organizers of short-course on Metabolic Phenotyping in Disease Diagnosis and Personalized Health Care at Imperial College United Kingdom are also highly appreciated.

Authors' Contributions
Sylvester Aghahowa: Designed the work for the PhD program and carried it out in all stages
Raymond Ozolua, Enitome Bafor, Ambrose Isah: Supervised the research at all stages
Philip Obarisiagbon, Paul Aikorogie: Involved in collection of blood extraction of sera samples
Michael Aghahowa, David Osifo: Funded part of the project and vetted the write-up

Ethical Approval
In this article, the animal regulations are followed as per the ethical committee guidelines of Department of Pharmacology and Toxicology, University of Benin, Nigeria and the University of Benin Teaching Hospital, Benin City, Nigeria; the authors observed the metabolomics of artemisinin-based combination therapies in experimental animals and humans. The collaborating centre was the Institute of Pharmacy and Biomedical Science, University of Strathclyde, Glasgow, United Kingdom. Ethical approval (ADM/E 22/A/VOL VII/1047) was obtained from the Animal Ethics Committee of the University of Benin, Nigeria for the animal-based studies. Also, the ethical approval (EC/FP/015/05) was sought and got from the University of Benin Teaching Hospital Benin City, Nigeria, for the human-based studies. The animal & human ethical guidelines are followed in the study for observation, identification & experimentation.

Informed Consent
Not applicable.

Conflicts of interests
The authors declare that they have no conflicts of interests, competing financial interests or personal relationships that could have influenced the work reported in this paper.

Funding
We wish to appreciate the supervisors and family members of the corresponding author for their financial support in the course of the study and did not receive any external funding.

Data and materials availability
The datasets generated and analyzed during the current study are not publicly available due bulky nature of information contained. All data will be made available on request from the corresponding author se-aghahowa@uniben.edu

REFERENCES

1. Aghahowa SE, Ozolua RI, Bafor EE, Obarisiagbon P, and Isah AO. Toxicity effect of ACTs plus paracetamol in malaria Patients. ToxicologicalReports, 2021;8:1930-1936.
2. Aghahowa SE, Obianwu HO, Isah AO. Tolerabilities of artemisinin-based combination drugs among patients with uncomplicated malaria in a tertiary institution Benin City. Nigerian. Journal of Clinical Pharmacology and Biopharmaceutics, 2014;3:2.
3. Aghahowa SE, Obianwu HO, Isah AO, Arhewoh MI. Possible mechanism, relevant factors and treatment approach of chloroquine-induced pruritus – a review. Indian Journal of Pharmaceutical Science, 2010;72(3):283-408.
4. Aprioku JS, and Obianime AW. Structure Activity – Relationship of Artemisinin on some Biological Systems in male Guinea pigs. Insight Pharmaceutical Science, 2011;1(1):1–10.

5. Bafor EE, Rowan EG, and Edrada-Ebel R. Toward Understanding Myometrial Regulation: Metabolomic Investigation Reveals New Pathways of Oxytocin and Ritodrine Activity on the Myometrium. Reproductive Science, 2017;24(5):691-705.
6. Bafor EE, Rowan EG, and Edrada-Ebel R. Metabolomics-Coupled Functional Pharmacology of Chlorophyll Compounds Isolated From the Leaves of Ficus Exasperata Vahl (Moraceae) Provides Novel Pathways on Myometrial Activity. Reproductive Science, 2018;25(6):923-937.
7. Bassi PU, Osakwe AI, Isah A, Suku C, Kalat JI, Wammanda RD, Ugochukwu C, Adesina O, Nyong EE, Osungwu F, Pal S, Nwoasu SC, Wallberg M, Coulter D. Safety of Artemisinin-Based Combination Therapies in Nigeria: A Cohort Event Monitoring Study. Drug Safety, 2013;17:11.15.
8. Beger R, Schnackenberg L, Holland R, Li D, Dragan Y. Metabonomic models of human pancreatic cancer using 1d proton NMR spectra of lipids in plasma. Metabolomics, 2006;2;125–134.
9. Boroujerdi AF, Vizcaino MI, Meyers A, Pollock EC, Huynh SL, Schock TB, Morris PJ, Bearden DW. NMR-based microbial metabolomics and the temperature-dependent coral pathogen Vibrio coralliilyticus. Environmental. Science. Technology, 2009;43:7658–7664.
10. Bouhifd M, Hartung T, Hogberg HT, Kleensang A, Zhao L. Review: Toxicometabolomics. Journal of Applied Toxicology, 2013;33:1365–1383.
11. Cheng C, MacIntyre L, Abdelmohsen UR, Horn H, Polymenakou PN, Edrada-Ebel R, Ute Hentschel. Biodiversity, Anti-Trypanosomal Activity Screening, and Metabolomic Profiling of Actinomycetes Isolated from Mediterranean Sponges. PLoS ONE. 2015;10(9):e0138528.
12. Dunn WB, Broadhurst D, Begley P, Zelena E, Francis-McIntyre S, Anderson N, Brown M, Knowles JD, Halsall A, Haselden JN, Nicholls AW, Wilson ID, Kell DB, Goodacre R, and The Human Serum Metabolome (HUSERMET) Consortium. Procedures for large-scale metabolic profiling of serum and plasma using gas chromatography and liquid chromatography coupled to mass spectrometry. Nature Protocol, 2011; 6(7):1061-1083.
13. Everett JR. Pharmacometabonomics in humans: a new tool for personalized medicine. Pharmacogenomics, 2015;16(7):737–754.
14. Falade C and Manyando C. Safety profile of Coartem®: the evidence base. Malaria Journal, 2009; (Suppl 1): S6. doi: 10.1186/1475-2875-8-S1-S6.
15. FMOH (Federal Ministry of Health Nigeria). National Antimalarial Treatment Policy, 2005;Pp 1-31.
16. Fidock DA, Rosenthal P, Croft SL, Brun R, and Nwaka S. Antimalarial drug discovery: Efficacy models for compound screening. Nature Review, 2004;3:911-916.
17. Fiehn O. Combining genomics, metabolome analysis, and biochemical modelling to understand metabolic networks. Computional Functional Genomics, 2001;2:155–168.
18. Flecknell P. Anesthesia of common laboratory species. In: Laboratory animal anesthesia. San Diego (CA): Academic Press, 1996;Pp 160–182.
19. Floegel A, Drogan D, Wang-Sattler R, Prehn C, Illig T, Adamski J, Hans-Georg Joost H, Boeing H, Pischon T. Reliability of Serum Metabolite Concentrations over a 4-Month Period Using a Targeted Metabolomic Approach. PLoS ONE, 2011;6(6):e21103. doi: 10.1371/journal.pone.0021103
20. Gardner MJ, Hall N, Fung E, White O, Berriman M, Hyman RW, Carlton JM, Pain A, Nelson KE, Bowman S, Paulsen IT, James K, Eisen JA, Rutherford K, Salzberg SL, Craig A, Kyes S, Chan MS, Nene V, Shallom SJ, Suh B, Peterson J, Angiuoli S, Pertea M, Allen J, Selengut J, Haft D, Mather MW, Vaidya AB, Martin DM, Fairlamb AH, Fraunholz MJ, Roos DS, Ralph SA, McFadden GI, Cummings LM, Subramanian GM, Mungall C, Venter JC, Carucci DJ, Hoffman SL, Newbold C, Davis RW, Fraser CM, Barrell B. Genome sequence of the human malaria parasite *Plasmodium falciparum*. Nature, 2002; 3;419(6906): 498-511.
21. Krettli A, Adebayo JO and Krettli LG. Testing of Natural Products and Synthetic Molecules Aiming at New Antimalarials. Current Drug Targets, 2009;10:261-270.
22. Li H, Tang H, and Wang Y, Advances in Metabonomics on Infectious Diseases. Current Metabolomics, 2013;1:318-334.
23. Macintyre L, Zhang T, Viegelmann C, Martinez IJ, Cheng C, Dowdells C, Abdelmohsen UR, Gernert C, Hentschel, U, Edrada-Ebel, R. Metabolomic tools for secondary metabolite discovery from marine microbial symbionts. Marine Drugs, 2014;12:3416–3448.
24. Mathur-De VR. The scope and limitations of a QA system in research. Accredited Quality Assurance, 2000;5:3–10.
25. McCarthy J, Loukas A, and Hotez PJ. Chemotherapy of Helminth Infections. Chemotherapy of Microbial Disease. In: L.L. Brunton, B.A. Chaber, B. C. Knollmann (Eds.): Goodman and Gilman's The Pharmacological Basis of Therapeutics, 12th ed., McGraw Hill, 2011;1443–62.
26. NIH (National Institute of Health). Guide for the Care and Use of Laboratory Animals. Committee for the Update of the Guide for the Care and Use of Laboratory Animals Institute for Laboratory Animal Research Division on Earth and Life Studies, 3rd Edition. The National academy Press, 2011; Pp 1-220.

27. Nicholson JK, Holmes E, Kinross JM, Darzi AW, Takat Z, Lindon JC. Metabolic phenotyping in clinical and surgical environments. Nature, 2012;491:384–392.
28. Nicholson JK, Lindon JC, Holmes E. "Metabonomics": understanding the metabolic responses of living systems to pathophysiological stimuli via multivariate statistical analysis of biological NMR spectroscopic data. Xenobiotica, 1999;29:1181–1189.
29. Olszewski KL, Morrisey JM, Wilinski D, Burns JM, Vaidya AB, Rabinowitz JD, Linas M. Host-Parasite interactions revealed by Plasmodium falciparum metabolomics. Cell Host Microbe, 2009; 5(2):191-199.
30. Parekh SB, Bubb WA, Hunt NH, Rae C. Brain metabolic markers reflect susceptibility status in cytokine gene knockout mice with murine cerebral malaria. International Journal of Parasitology, 2006; 36(13):1409-1418.
31. Rang HP, Dale MM, Ritter JM. Flower RJ, Henderson G. Pharmacology. Seventh Edition Elsevier Churchill Livingstone. 2012, Pp 1-777.
32. Sana TR, Gordon DB, Fischer SM, Tichy SE, Kitagawa N, Lai C, Gosnell WL, Chang SP. Global mass spectrometry-based metabolomics profiling of erythrocytes infected with Plasmodium falciparum. PloS One, 2013;8(4):e60840.
33. Tsang TM, Woodman B, Mcloughlin GA, Griffin JL, Tabrizi SJ, Bates GP, Holmes E. Metabolic characterization of the R6/2 transgenic mouse model of Huntington's disease by high-resolution MAS 1H NMR spectroscopy. Journal of Proteome Research, 2006;5:483–492.
34. Want EJ, O'Maille G, Smith CA, Brandon TR, Uritboonthai W, Qin C, Trauger SA, and Siuzdak, G. Solvent-Dependent Metabolite Distribution, Clustering, and Protein Extraction for Serum Profiling with Mass Spectrometry. Analytical. Chemistry, 2006;78,3(1):743-752.
35. WHO. Antimalarial Drug Combination therapy: Report of a WHO Technical Consultation. Geneva. World Health Organization, WHO\CDS\RMB\2001. 1-36.
36. WHO. Relationship between sample size and probability of observing an adverse event (AE). A practical handbook on the pharmacovigilance of antimalarial medicines. W.H. O. press 2007, Pp 27.
37. WHO. Guidelines for the treatment of malaria 2nd edition, 2010, Pp 1-88.
38. WHO. World Malaria Report. http://www.who.int/malaria/publications/worldmalaria-report-2013/en/index.Pp 1-286.
39. Wishart DS, Tzur D, Knox C, Eisner R, Guo AC, Young N, Cheng D, Jewell K, Arndt D, Sawhney S, Fung C, Nikolai L, Lewis M, Coutouly MA, Forsythe I, Tang P, Shrivastava S, Jeroncic K, Stothard P, Amebey G, Block D, Hau DD, Wagner J, Miniaci J, Clements M, Gebremedhin M, Guo N, Zhang Y, Duggan GE, Macinnis GD, Weljie AM, Dowlatabadi R, Bamforth F, Clive D, Greiner R, Li L, Marrie T, Skyes BD, Vogel HJ, Querengeser L. HMDB: the human metabolome database. Nucleic Acids Research, 2007;35:D521-D6.
40. Xie LH, Li Q, Lin AJ, Smith K, Zhang J, and Skillman DS. New potential Antimalarial Agents: Therapeutic-index evaluation of Pyrroloquinazolinediamine and its pro-drug in a rat model of severe Malaria. Antimicrobial Agents of Chemotherapy, 2006;50(5):1649-1655.
41. Zhang S, Nagana GA, Asiago V, Shanaiah N, Barbas C, Raftery D. Correlative and quantitative 1H NMR-based metabolomics reveals specific metabolic pathway disturbances in diabetic rats. Annals of Biochemistry, 2008;1; 383(1):76-84.
42. Zimmerman H. Hepatotoxicity: The Adverse Effects of Drugs and Other Chemicals on the Liver, 2nd ed. Lippincott Williams & Wilkins, Philadelphia PA. 1999, Pp 76.